

Computationally Generated Charts for Critical Local Buckling Stress of L-, T-, and Cruciform-Section Columns

Joshua F. Griffin¹

Mississippi State University, Starkville, MS, 39762, USA

When performing hand calculations for critical local buckling stresses, charts are commonly used to determine the coefficient in the governing equation. Historically, these values have been calculated using moment-distribution methods supplemented by energy methods, often through manual means. This paper discusses the computational implementation of moment-distribution methods, significantly reducing the need for energy methods due to increased computing power. Considerations for ensuring that assumptions fall within appropriate ranges for accurate moment-distribution calculations are discussed. The accuracy of the computational approach is validated by comparing computed values in regions where energy methods were traditionally used against historical data for Z-stringers. Charts for determining critical local buckling stresses of columns with L-, T-, and cruciform cross-sections are presented. The application of moment-distribution methods to these geometries is detailed, and the computed results are validated against finite element simulations performed in Abaqus.

I. Nomenclature

σ	=	compressive stress
k	=	local buckling coefficient
E	=	modulus of elasticity
ν	=	Poisson's ratio
t	=	thickness
b	=	length of a loaded edge of a plate or flange
ϵ	=	rotation restraint coefficient
λ	=	half-wavelength of the local instability
f	=	flange
w	=	web
U	=	modified stiffness stability factor
S	=	stiffness
D	=	$\frac{Eh^3}{12(1-\nu^2)}$, flexural rigidity

II. Introduction

Mass efficiency is critical in flight vehicle structures and is often achieved using thin skin stiffened by stringers. When analyzing stringer-stiffened panels, the local buckling stress of the stringers is often of interest. To calculate the elastic local buckling stress, an adaptation of the plate buckling equation, Eq. (1), can be used [1].

$$\sigma = \frac{k\pi^2 E}{12(1-\nu^2)} \left(\frac{t}{b}\right)^2 \quad (1)$$

¹Undergraduate Senior, Department of Aerospace Engineering, Mississippi State, and AIAA Student Member 1799398.

Where t and b are the thickness and length, respectively, of an element of the stringer cross-section. The buckling coefficient, k , depends on the geometry of the structure [2]. For simple cases, k can be determined analytically, but for stringers, interdependent structural elements create unknown rotational restraints, making direct calculation unsolvable [1].

To address this, Lundquist, Stowell, and Schuette [1], developed an iterative method, solving equilibrium equations for various instability wavelengths to determine the lowest-energy buckling mode. Historically, this process was computationally intensive and feasibly limited to common stringer geometries [2], with some values supplemented using energy methods. Advances in computing now allow moment-distribution methods to generate additional charts for hand-sizing calculations of local buckling.

This paper presents computationally generated charts for the critical local buckling stress of L-, T-, and cruciform-section columns. The implementation of moment-distribution methods is discussed, along with considerations for assumption validity. Results are validated against historical Z-stringer data [2] and finite element simulations in Abaqus.

III. Procedure

The moment-distribution method was implemented computationally using a C program to generate charts for the critical local buckling stress of Z-, L-, T-, and cruciform-section columns. The column cross-sections used in this study are shown in Fig. 1. The dimensions were defined such that $t_{f1} = t_{f3}$, $t_{f2} = t_{f4}$, $b_{f1} = b_{f3}$, $b_{f2} = b_{f4}$, where t is the thickness of a column element and b is the length of a loaded edge. Subscripts f and w denote flanges and webs, respectively.

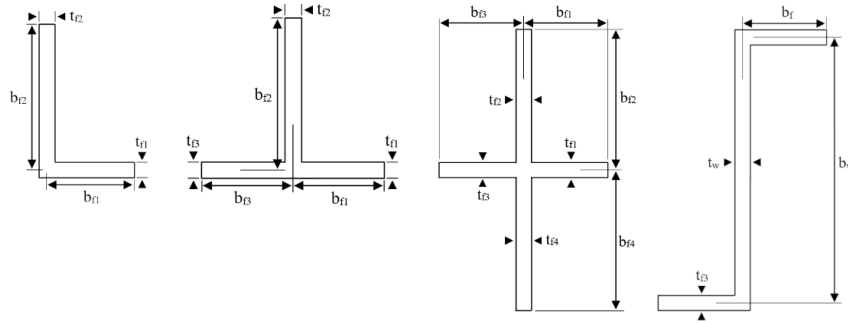


Fig. 1 Column Section Geometries

A. Formulation of Moment-distribution Equations

Equations were derived for each column geometry in terms of the modified stiffness stability factor, U . Literature describing the formulation of these equations in the manner of Lundquist, Stowell, and Schuette [1] is scarce. However, by analyzing Eq. (2a) for Z- and C-sections [1] and equations from previous studies [2][3], and comparing their results with adjacent methods, trends were identified. Using these observed behaviors, the new equations governing L-, T-, and cruciform-section columns were developed, Eq. (2b)-(2d).

$$U_Z = \left(\frac{S^3 b}{D}\right)_f + \left(\frac{S^4 b}{D}\right)_w \left(\frac{t_w}{t_f}\right)^3 \left(\frac{b_f}{b_w}\right) \quad (2a)$$

$$U_L = \left(\frac{S^3 b}{D}\right)_{f1} + \left(\frac{S^3 b}{D}\right)_{f2} \left(\frac{t_{f2}}{t_{f1}}\right)^3 \left(\frac{b_{f1}}{b_{f2}}\right) \quad (2b)$$

$$U_T = \left(\frac{S^3 b}{D}\right)_{f1} + 2 \left(\frac{S^3 b}{D}\right)_{f2} \left(\frac{t_{f2}}{t_{f1}}\right)^3 \left(\frac{b_{f1}}{b_{f2}}\right) \quad (2c)$$

$$U_{Cruciform} = 2 \left(\frac{S^3 b}{D}\right)_{f1} + 2 \left(\frac{S^3 b}{D}\right)_{f2} \left(\frac{t_{f2}}{t_{f1}}\right)^3 \left(\frac{b_{f1}}{b_{f2}}\right) \quad (2d)$$

Where D is the flexural rigidity of the column element, and S is the stiffness, which relates the moment per unit length per quarter-radian rotations at the edge of a column element [1]. The stiffness term varies based on the condition given to the far edge of the column element. In Eqs. (2a)-(2d), S^3 is for free edges, and S^4 is for an element about

symmetry in the cross-section [1]. These terms are derived in Ref. [1] and are described in Eqs. (3a)-(4d). Poisson's ratio, ν , was assumed to be 0.3, consistent with prior studies [1].

$$\frac{S^3b}{D} = \left[\left(\frac{\alpha}{2} \right)^2 + \left(\frac{\beta}{2} \right)^2 \right] \left[\frac{\frac{\beta}{2}m^2(1-\tan^2\frac{\beta}{2})\tanh\frac{\alpha}{2}-\frac{\alpha}{2}n^2(1+\tanh^2\frac{\alpha}{2})\tan\frac{\beta}{2}}{\frac{mn\alpha\beta}{2\cosh^2\frac{\alpha}{2}\cos^2\frac{\beta}{2}}+\frac{\alpha\beta}{4}(m^2+n^2)(1+\tanh^2\frac{\alpha}{2})(1-\tan^2\frac{\beta}{2})+4\left[\left(\frac{m\beta}{2}\right)^2+\left(\frac{n\alpha}{2}\right)^2\right]\tanh\frac{\alpha}{2}\tan\frac{\beta}{2}} \right] \quad (3a)$$

$$\frac{S^4b}{D} = \frac{\frac{1}{2}\left[\left(\frac{\alpha}{2}\right)^2+\left(\frac{\beta}{2}\right)^2\right]}{\frac{\alpha}{2}\tanh\frac{\alpha}{2}+\frac{\beta}{2}\tan\frac{\beta}{2}} \quad (3b)$$

$$\alpha = \pi\sqrt{\frac{b}{\lambda}}\sqrt{\sqrt{k}+\frac{b}{\lambda}} \quad (4a)$$

$$\beta = \pi\sqrt{\frac{b}{\lambda}}\sqrt{\sqrt{k}-\frac{b}{\lambda}} \quad (4b)$$

$$m = \left(\frac{\alpha}{2}\right)^2 - \nu\left(\frac{\pi b}{2\lambda}\right)^2 \quad (4c)$$

$$n = \left(\frac{\beta}{2}\right)^2 + \nu\left(\frac{\pi b}{2\lambda}\right)^2 \quad (4d)$$

To satisfy the stability criterion, U , was set to zero in the governing equations, following the approach of Lundquist, Stowell, and Schuette [1], as shown in Eqs. (5a)-(5d). Notably, this simplification results in equivalent buckling coefficients for L- and cruciform-section columns.

$$\left[0 = \left(\frac{S^3b}{D}\right)_f + \left(\frac{S^4b}{D}\right)_w \left(\frac{t_w}{t_f}\right)^3 \left(\frac{b_f}{b_w}\right) \right]_Z \quad (5a)$$

$$\left[0 = \left(\frac{S^3b}{D}\right)_{f1} + \left(\frac{S^3b}{D}\right)_{f2} \left(\frac{t_{f2}}{t_{f1}}\right)^3 \left(\frac{b_{f1}}{b_{f2}}\right) \right]_L \quad (5b)$$

$$\left[0 = \left(\frac{S^3b}{D}\right)_{f1} + 2\left(\frac{S^3b}{D}\right)_{f2} \left(\frac{t_{f2}}{t_{f1}}\right)^3 \left(\frac{b_{f1}}{b_{f2}}\right) \right]_T \quad (5c)$$

$$\left[0 = 2\left(\frac{S^3b}{D}\right)_{f1} + 2\left(\frac{S^3b}{D}\right)_{f2} \left(\frac{t_{f2}}{t_{f1}}\right)^3 \left(\frac{b_{f1}}{b_{f2}}\right) \right]_{Cruciform} \quad (5d)$$

B. Numerical Computation and Chart Generation

A range of assumed values for λ/b_{f1} , the ratio of half-wavelength to flange length, was used in the calculations, ranging from $\lambda/b_{f1} = 1$ to $\lambda/b_{f1} = 2,000$. For each assumption of λ/b , the correct buckling coefficient k was determined by identifying the lowest value of k satisfying its respective equation from Eqs. (5a)-(5d). The assumption providing the lowest value of k corresponds to the lowest-energy mode of local buckling. This process is described in detail in Ref. [1].

The C program implemented these equations to compute k values across a practical range of flight-vehicle structural dimensions. The analyzed parameter ranges included the following:

1. Thickness ratios t_{f2}/t_{f1} or t_w/t_f , from 0.5 to 2.0 in increments of 0.1.
2. Length ratios b_{f1}/b_{f2} or b_f/b_w , from 0.05 to 2.0 in increments of 0.05

The resulting values of k are tabulated in Tables 1 - 3 in the Appendix. Additionally, for completeness and consistency with previous works [1][2], an extra data point ($b_{f1}/b_{f2} = 0$, $k = 0.428858$) was included in the charts created for this paper. This point represents the buckling coefficient for a simply supported flange accommodating an infinite value of λ/b . The value for this was determined by taking the limit of the equation determined by Lindquist and Stowell [4] for flange buckling with $\varepsilon = 0$. However, in reality, if b_{f1}/b_{f2} or b_f/b_w equals zero, the flange does not exist. Therefore, the flange cannot provide the minimum assumed simply support boundary condition, and the structure would instead globally buckle as a plate with both unloaded edges free.

In addition to determining the critical local buckling stress, it is also important to identify the specific part of the column undergoing local buckling. For the geometries historically addressed in buckling charts, this involved analyzing the signs of terms in the equilibrium equations, such as Eq. (5a) [2]. However, L-, T-, and cruciform sections, as discussed in this paper, are composed entirely of flanges. This leads to the conclusion that the flanges will simultaneously experience local buckling when they are constrained to a simply supported condition relative to each other [7, pp. C6.1]. As previously noted, at this point, $k = 0.428858$. Therefore, a dashed line has been added to the final charts to identify this value. These final charts, plotted in MATLAB [6], along with the graphics from Fig. 1, are presented in Figs. 7-8 in the Appendix. For the charts, the values of k_{f2} were gained from Eq. (6) and used instead of k_{f1} , in accordance with the charts commonly used in aerostructural analysis literature [7, pp. C6.3], and should be applied to Eq. (7).

$$k_{f2} = \frac{k_{f1}}{\left(\frac{t_{f2}b_{f1}}{t_{f1}b_{f2}}\right)^2} \quad (6)$$

$$\sigma = \frac{k_{f2}\pi^2 E}{12(1-\nu^2)} \left(\frac{t_{f2}}{b_{f2}}\right)^2 \quad (7)$$

C. Finite Element Analysis in Abaqus

To validate the data obtained from moment-distribution methods, finite element analysis was performed in Abaqus Learning Edition [5] for L-, T-, and cruciform-section columns. The material was given a Young's Modulus of 10.6×10^6 psi, and a Poisson's Ratio of 0.3. The columns were modeled as follows:

1. The columns were 10 inches long.
2. Flanges $f2$ and $f4$ were 1 inch in length in all scenarios.
3. Flanges $f1$ and $f3$ were varied to achieve the desired values of b_{f1}/b_{f2} .

A shell extrusion method was used to minimize node count, as Abaqus Learning Edition is limited to 1000 nodes [5]. Section assignments were applied to achieve the equivalent thickness ratios. A unit load was applied at the geometric center of the column using a reference point constrained to the nodes at that end. Boundary conditions included:

1. For the loaded end, displacement allowed only in the load direction, constrained in all other directions.
2. The unloaded end was simply supported.
3. The edge where flanges meet was constrained just as the loaded end to prevent global buckling and isolate local buckling

Figure 2 shows the boundary conditions and unit load in Abaqus. An eigenvalue buckling analysis was performed, and the first eigenvalue was recorded as the critical local buckling load. The results were compared with values obtained from moment-distribution methods and are summarized in Table 5 of the Appendix.

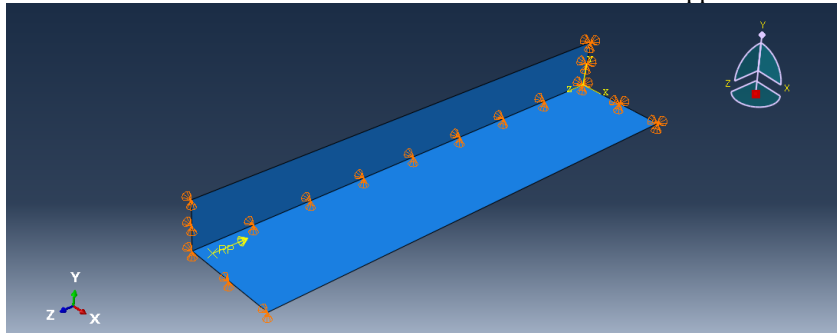


Fig. 2 Boundary Conditions and Unit Load in Abaqus

IV. Discussion

Figs. 7-8 presented in this paper utilize values obtained through the moment-distribution method in regions where, historically, energy methods have been employed. These regions typically correspond to low values of t_2/t_1 or t_w/t_f ,

generally less than 0.25, and for some column geometries, less than 1.0 [2]. To validate that the moment-distribution method can yield results consistent with energy methods in these regions, the data from this paper is compared with that from Ref. [2], where it was obtained using energy methods. The trends observed in Fig. 3 are nearly identical.

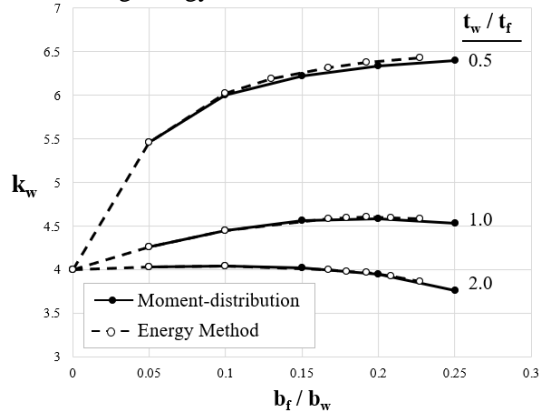


Figure 3. Values of k by Moment-distribution and Energy Methods for Z- section.

When performing moment-distribution method calculations, several behaviors can lead to errors if not properly accounted for in programming. Specifically, when determining the correct value of k for a given assumption of λ/b , Eqs. (5a)- (5c) exhibit discontinuous behaviors, resulting in multiple values of k that satisfy $U = 0$, as shown in Fig. 4. This issue can be addressed programmatically by implementing a search pattern that starts at zero and progresses with appropriate fidelity. For the data presented in this paper, an initial step size of 10^{-3} was used to find an approximate solution, which was then refined with a step size of 10^{-5} . Upon reflection, a step size of 10^{-2} could be appropriate and more efficient.

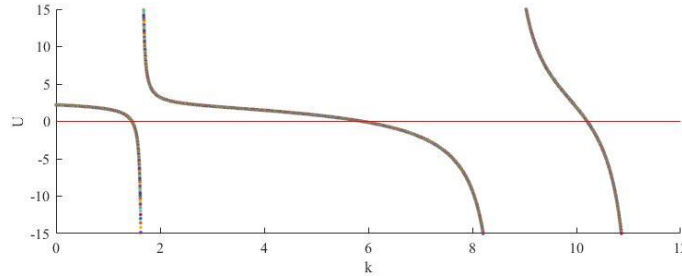


Figure 4. Behavior of U Equilibrium Equation for Z- section with $t_w/t_f = 1.0$ & $b_f/b_w = 1.0$.

An additional behavior occurs in the next step of the moment-distribution method, after the correct value of k for each assumption of λ/b has been found, where the lowest value of all the k values is being determined. In L-, T-, and cruciform sections, it was observed that k exhibits two distinct patterns in relation to λ/b . The first pattern, shown in Fig. 5(a), demonstrates that k approaches its lowest value as λ/b increases toward infinity. The second pattern, shown in Fig. 5(b), indicates that k dips initially, then increases and approaches a value higher than its lowest point as λ/b reaches infinity. A similar behavior with different patterns was also observed in Z- and C-sections.

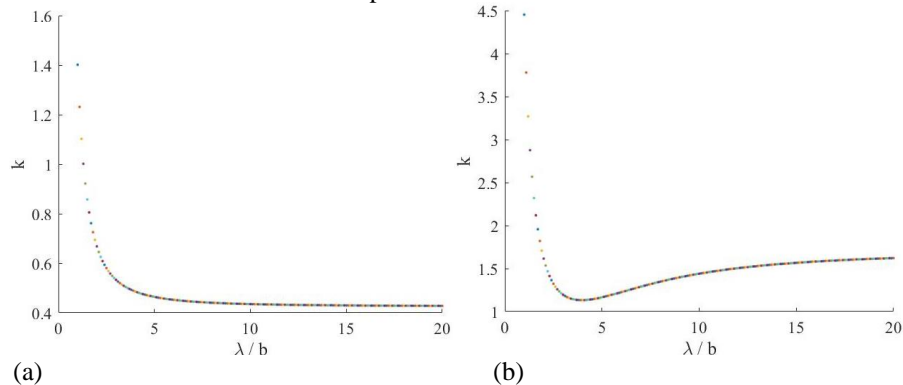


Figure 5. Behavior of k Against λ/b for L- section, (a) $t_{f2}/t_{f1} = 1.0$ & $b_{f1}/b_{f2} = 1.0$, (b) $t_{f2}/t_{f1} = 0.5$ & $b_{f1}/b_{f2} = 0.5$.

Comparison between the values for k achieved by moment-distribution methods and by simulation are included in Table 5 of the Appendix and presented in Figs. 6(a)-7(c). The magnitudes of errors range from 0.1231% to 17.04%, and the average magnitude of the percentage error is 4.586%.

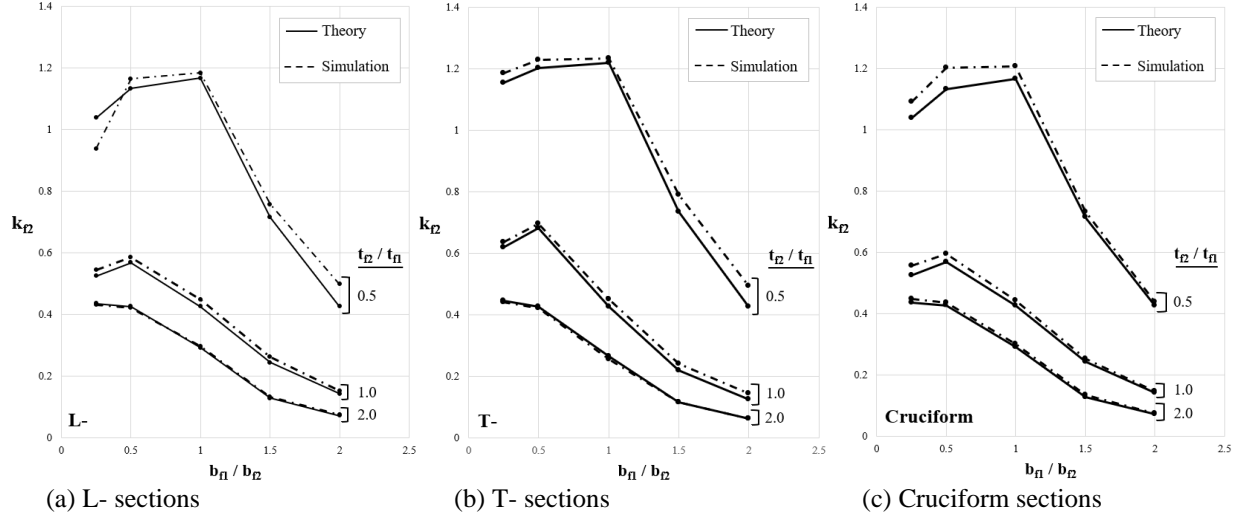


Figure 6. Comparison Between Moment-distribution and FEA Simulations.

All points where the error between the moment-distribution method and simulation exceeded 10% occurred at $b_{f1}/b_{f2} = 2$. These points correspond to $t_{f2}/t_{f1} = 0.5$ for L- and T- sections, and $t_{f2}/t_{f1} = 1.0$ for T- sections. These three points exhibited the form where the lowest value of k was found as λ/b_{f1} approached infinity (Fig. 5(a)), such that the column length was shorter than the half-wavelength, λ , at which local buckling would initially occur. While other points shared this form, the three points at $b_{f1}/b_{f2} = 2$ were generated in Abaqus by increasing the length of flange $f1$. This led to a relative column length that was insufficient to accommodate a local instability of the expected length λ . As a result, the local instability occurred at a smaller wavelength, which increased the critical stress for local buckling. Fortunately, this is a conservative behavior. In application, this behavior, when occurring, can be corrected by using the length of the given column for λ in Eqs. (4a)-(4d) and solving for a unique value of k .

Additionally, an error of -9.594% is observed in the L-section data where $t_{f2}/t_{f1} = 0.5$ and $b_{f1}/b_{f2} = 0.25$. Using a method outlined by Bruhn [7, pp. C7.6], where Eq. (8) must be satisfied, it was determined that, in this case, flange $f1$ is not large enough to provide the minimum simply supported condition assumed by the moment-distribution method for flange $f2$. As a result, buckling in this geometric configuration behaves more like a plate with both unloaded edges free.

$$2.73 \frac{I_{f1}}{b_{f2} t_{f2}^3} - \frac{A_{f1}}{b_{f2} t_{f2}} \geq 5 \quad (8)$$

Because the behavior of these four points can be explained, these outliers can be removed from the consideration of the error, and the average magnitude of the percentage error is now 3.606%.

V. Conclusion

Charts to assist in determining the critical local buckling stress of L-, T-, and cruciform sections columns are included in the Appendix in Figs. 7-8 and should be used with Eq. (7). Users of these charts should verify that the flanges of the columns can reciprocally provide a simply supported boundary condition. The stress calculated from this equation is of course, the elastic stress, and a plasticity correction should be done if necessary.

$$\sigma = \frac{k_{f2} \pi^2 E}{12(1-\nu^2)} \left(\frac{t_{f2}}{b_{f2}} \right)^2 \quad (7)$$

Appendix

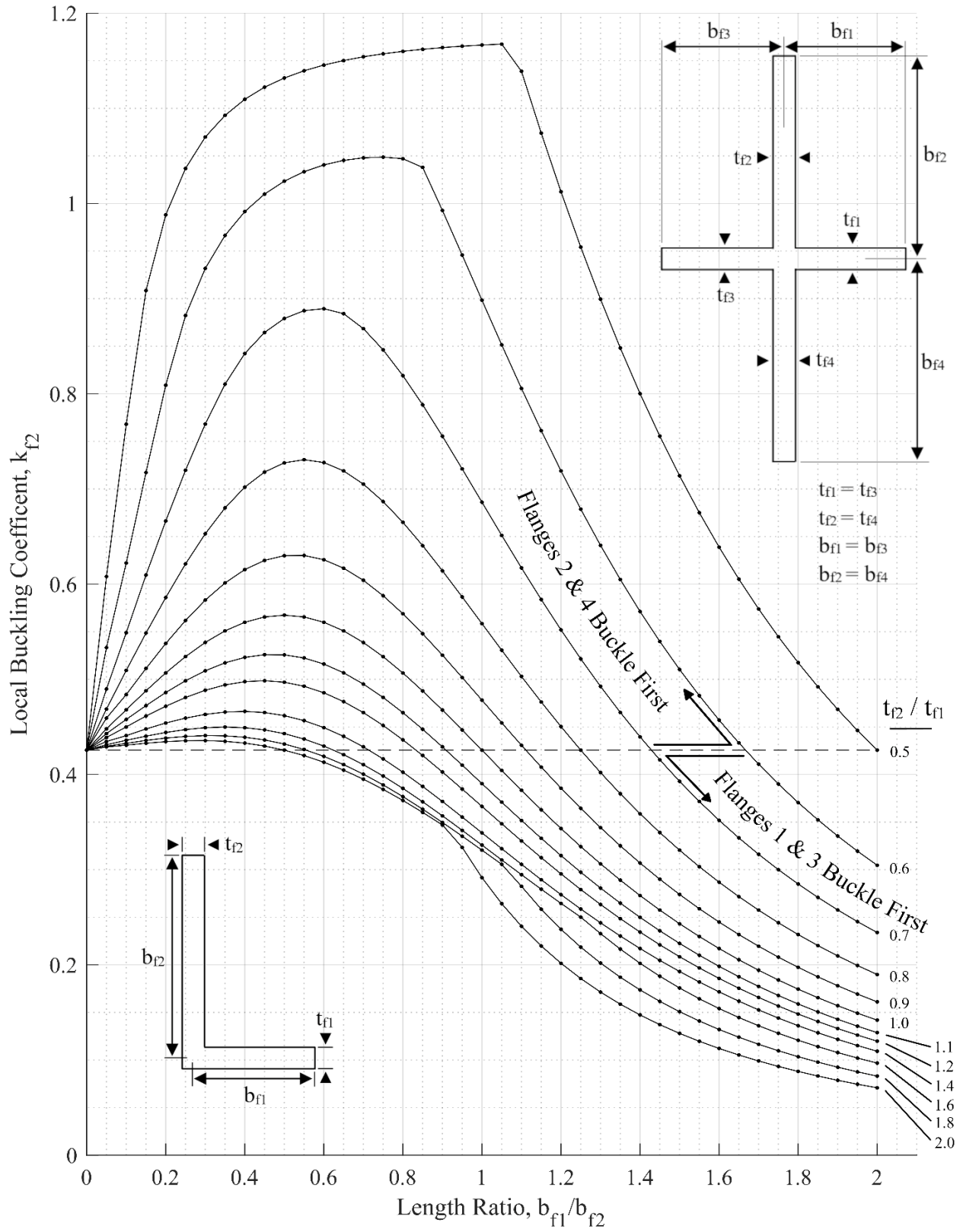


Figure 7. Chart for Buckling Coefficient of L- and Cruciform Section Columns

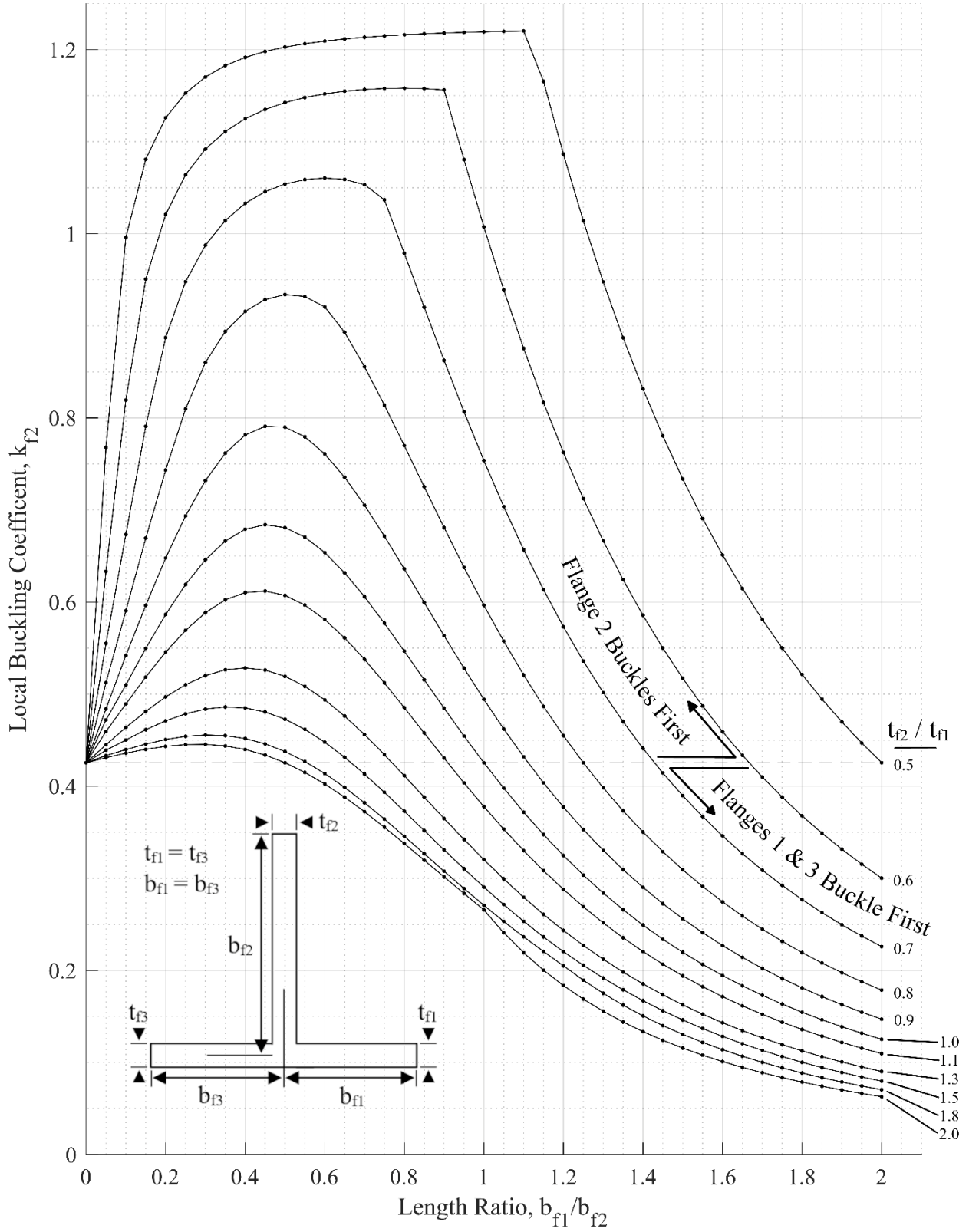


Figure 8. Chart for Buckling Coefficient of L- and Cruciform Section Columns

Table 3. Values of k_w from Moment-distribution for Z- Section Columns

t_w/t_f b_f/b_w	t_w/t_f															
	0.5	0.6	0.7	0.8	0.9	1	1.1	1.2	1.3	1.4	1.5	1.6	1.7	1.8	1.9	2
0.05	5.456000	5.000000	4.685714	4.481250	4.350617	4.260000	4.195041	4.152778	4.120710	4.095918	4.078222	4.064062	4.052595	4.044444	4.037673	4.032000
0.1	6.004000	5.536111	5.128571	4.821875	4.603704	4.450000	4.339669	4.260417	4.202367	4.159184	4.126222	4.101172	4.081315	4.065741	4.053463	4.043500
0.15	6.222222	5.817284	5.392290	5.032639	4.759945	4.560000	4.415060	4.309259	4.231164	4.173016	4.128988	4.095486	4.069512	4.049246	4.033241	4.020556
0.2	6.333000	5.965278	5.532653	5.137500	4.822531	4.586750	4.413636	4.287153	4.193639	4.124107	4.071556	4.031641	4.000865	3.976852	3.957895	3.942750
0.25	6.393600	6.044889	5.594449	5.157000	4.799012	4.528960	4.330182	4.184333	4.076213	3.994857	3.932729	3.884187	3.845260	3.813086	3.785573	3.760960
0.3	6.429333	6.086728	5.597959	5.096701	4.685460	4.377667	4.151423	3.983410	3.855819	3.755669	3.673679	3.602778	3.537370	3.472188	3.400800	3.267306
0.35	6.451592	6.104082	5.539359	4.936352	4.463794	4.118286	3.863046	3.668084	3.511798	3.378384	3.255619	3.132462	2.995805	2.823684	2.613896	2.400673
0.4	6.465750	6.102257	5.361097	4.639160	4.124691	3.754625	3.476808	3.256163	3.068602	2.897066	2.728694	2.554150	2.370437	2.184510	2.006492	1.838328
0.45	6.475259	6.070096	4.967196	4.217901	3.703643	3.331802	3.046424	2.812689	2.608342	2.419224	2.237564	2.061150	1.891973	1.733425	1.587784	1.452938
0.5	6.481600	5.537667	4.451837	3.749437	3.265284	2.910200	2.632826	2.402333	2.200355	2.016449	1.845867	1.687328	1.541218	1.408025	1.287668	1.177400
0.55	6.485950	4.908173	3.933952	3.299535	2.857300	2.528694	2.269162	2.052663	1.864169	1.695530	1.542744	1.404145	1.278881	1.166259	1.065397	0.973628
0.6	5.747000	4.325077	3.463832	2.897917	2.499348	2.200278	1.962603	1.764371	1.593064	1.441752	1.306778	1.186024	1.078133	0.981919	0.896253	0.818715
0.65	5.061680	3.814924	3.054752	2.551257	2.193703	1.923503	1.708035	1.528583	1.374462	1.239609	1.120494	1.014922	0.921275	0.838235	0.764589	0.688201
0.7	4.475020	3.377664	2.704748	2.256091	1.935349	1.691755	1.497082	1.335232	1.196921	1.076687	0.971256	0.878388	0.796455	0.724080	0.660099	0.602607
0.75	3.976391	3.005235	2.406785	2.005611	1.717289	1.497476	1.321594	1.175580	1.051277	0.943782	0.849999	0.767785	0.695529	0.631907	0.575763	0.525507
0.8	3.552437	2.687977	2.153029	1.792773	1.532716	1.333875	1.174638	1.042632	0.930594	0.834072	0.750208	0.676959	0.612776	0.556399	0.506761	0.462402
0.85	3.190754	2.416801	1.936134	1.611159	1.375710	1.195266	1.050668	0.930950	0.829574	0.742532	0.667134	0.601476	0.544079	0.493767	0.449539	0.410104
0.9	2.880543	2.183916	1.749887	1.455382	1.241381	1.077049	0.945291	0.836317	0.744247	0.665382	0.597246	0.538055	0.486424	0.441232	0.401566	0.366272
0.95	2.613097	1.982825	1.589033	1.321001	1.125734	0.975512	0.855054	0.755502	0.671534	0.599768	0.537898	0.484262	0.437554	0.396734	0.360949	0.329158
1	2.381120	1.808250	1.449367	1.204422	1.025556	0.887760	0.777231	0.685951	0.609083	0.543500	0.487071	0.438230	0.395768	0.358710	0.326241	0.297458
1.05	2.178830	1.655858	1.327428	1.102721	0.938272	0.811438	0.709664	0.625687	0.555048	0.494882	0.443203	0.398537	0.359755	0.325948	0.296352	0.270166
1.1	2.001455	1.522107	1.220391	1.013494	0.861790	0.744653	0.650652	0.573123	0.507991	0.452593	0.405073	0.364063	0.328497	0.297523	0.270429	0.246494
1.15	1.845142	1.404117	1.125960	0.934806	0.794418	0.685905	0.598797	0.527006	0.466751	0.415570	0.371724	0.333929	0.301183	0.272695	0.247791	0.225826
1.2	1.706667	1.299537	1.042248	0.865093	0.734774	0.633937	0.553002	0.486318	0.430408	0.382972	0.342377	0.307425	0.277179	0.250883	0.227909	0.207674
1.25	1.583488	1.206436	0.967719	0.803040	0.681711	0.587770	0.512349	0.450240	0.398213	0.354113	0.316416	0.283995	0.255960	0.231609	0.210347	0.191645
1.3	1.473420	1.123192	0.901051	0.747550	0.634305	0.546550	0.476092	0.418097	0.369549	0.328442	0.293341	0.263175	0.237116	0.214495	0.194758	0.177413
1.35	1.374661	1.048453	0.841208	0.697745	0.591780	0.509602	0.443619	0.389331	0.343923	0.305504	0.272729	0.244588	0.220297	0.199229	0.180854	0.164723
1.4	1.285735	0.981108	0.787255	0.652870	0.553477	0.476357	0.414416	0.363485	0.320909	0.284920	0.254243	0.227926	0.205227	0.185551	0.168400	0.153357
1.45	1.205346	0.920201	0.738470	0.612292	0.518859	0.446321	0.388062	0.340170	0.300167	0.266376	0.237599	0.212929	0.191667	0.173246	0.157201	0.143138
1.5	1.132462	0.864951	0.694195	0.575472	0.487462	0.419098	0.364191	0.319068	0.281402	0.249612	0.222556	0.199382	0.179419	0.162137	0.147091	0.133912
1.55	1.066156	0.814649	0.653885	0.541955	0.458900	0.394343	0.342494	0.299905	0.264372	0.234401	0.208914	0.187102	0.168322	0.152072	0.137932	0.125557
1.6	1.005656	0.768739	0.617084	0.511359	0.432832	0.371766	0.322721	0.282444	0.248863	0.220558	0.196507	0.175931	0.158232	0.142924	0.129611	0.117965
1.65	0.950288	0.726712	0.583392	0.483351	0.408974	0.351115	0.304639	0.266491	0.234700	0.207922	0.185183	0.165744	0.149030	0.134585	0.122025	0.111046
1.7	0.899516	0.688139	0.552461	0.457639	0.387086	0.332173	0.288067	0.251874	0.221730	0.196356	0.174822	0.156426	0.140616	0.126958	0.115091	0.104722
1.75	0.852807	0.652644	0.524002	0.433985	0.366952	0.314756	0.272837	0.238449	0.209822	0.185739	0.165316	0.147878	0.132900	0.119968	0.108736	0.098927
1.8	0.809765	0.619916	0.497745	0.412167	0.348384	0.298704	0.258805	0.226085	0.198862	0.175975	0.156573	0.140019	0.125808	0.113543	0.102895	0.093601
1.85	0.769987	0.589660	0.473475	0.391997	0.331229	0.283874	0.245848	0.214674	0.188751	0.166967	0.148514	0.132777	0.119273	0.107626	0.097516	0.088697
1.9	0.733152	0.561634	0.450992	0.373316	0.315338	0.270147	0.233859	0.204119	0.179400	0.158642	0.141066	0.126085	0.113239	0.102160	0.092551	0.084170
1.95	0.698982	0.535620	0.430120	0.355971	0.300592	0.257412	0.222739	0.194337	0.170739	0.150932	0.134171	0.119893	0.107655	0.097105	0.087957	0.079983
2	0.667230	0.511431	0.410704	0.339844	0.286880	0.245575	0.212411	0.185250	0.162697	0.143777	0.127776	0.114149	0.102476	0.092417	0.083699	0.076103

Table 4. Values of k_w from Moment-distribution and Energy Methods for Z- Section Columns

t_w/t_f b_f/b_w	t_w/t_f										
	0.5	0.6	0.7	0.8	0.9	1	1.2	1.4	1.6	1.8	2
0.000	4.00	0.70	-	-	-	4.00	-	-	-	-	4.00
0.050	5.46	-	-	-	-	4.26	-	-	-	-	4.03
0.100	6.02	-	-	-	-	4.45	-	-	-	-	4.04
0.130	6.19	-	-	-	-	-	-	-	-	-	-
0.167	6.31	-	-	-	-	4.58	-	-	-	-	4.00
0.179	-	-	-	-	-	4.59	-	-	-	-	3.98
0.192	6.38	-	-	-	-	4.60	-	-	-	-	3.97
0.208	-	-	-	-	-	4.59	-	-	-	-	3.92
0.227	6.43	-	-	-	-	4.58	-	-	-	-	3.86
0.250	-	6.03	5.59	5.15	4.79	4.58	4.19	4.00	3.88	3.81	3.76
0.300	5.50	6.10	5.59	5.12	4.69	4.41	3.98	3.76	3.59	3.48	3.26
0.350	-	6.13	5.55	4.92	4.46	4.11	3.65	3.36	3.13	2.78	2.41
0.400	6.53	6.11	5.36	4.62	4.09	3.74	3.25	2.89	2.56	2.18	1.87
0.450	-	6.06	4.93	4.19	3.70	-	-	-	-	-	-
0.475	-	5.86	-	-	-	-	-	-	-	-	-
0.500	6.54	5.46	4.43	3.74	3.26	2.90	2.40	2.02	1.69	1.42	1.19
0.525	6.54	-	-	-	-	-	-	-	-	-	-
0.550	6.46	-	-	-	-	-	-	-	-	-	-
0.560	6.00	-	-	-	-	-	-	-	-	-	-
0.575	6.07	-	-	-	-	-	-	-	-	-	-
0.600	5.70	4.31	3.46	2.91	2.49	2.20	1.76	1.44	1.19	0.98	0.83
0.700	4.45	3.36	2.73	2.27	1.93	1.70	1.32	1.09	0.89	0.72	-
0.800	3.54	2.68	2.16	1.77	1.53	1.36	1.05	0.84	0.67	0.55	0.45
1.000	2.39	1.81	1.44	1.21	1.03	0.89	0.68	0.55	0.44	0.36	0.30

(Source: Adapted from [2].)

Table 5. Results from Abaqus Simulation and Comparison to Moment-distribution Theory

stringer type	Geometry								Simulation Results			Theory Results		Error (%)
	t_1 (in)	t_2 (in)	t_2/t_1	b_f1 (in)	b_f2 (in)	b_f1/b_f2	Area (in ²)	load (lb)	stress (psi)	k_f2	k_f2	(Sim - Theory) / Theory		
L	0.2	0.1	0.5	0.25	1	0.25	0.13	11674	89800	0.937331828	1.0368	-9.593766543		
	0.2	0.1	0.5	0.5	1	0.5	0.18	20060	111444.4444	1.163256402	1.13184	2.77569284		
	0.2	0.1	0.5	1	1	1	0.28	31718	113278.5714	1.182401008	1.16648	1.364876176		
	0.2	0.1	0.5	1.5	1	1.5	0.38	27550	72500	0.756754539	0.713831	6.013123356		
	0.2	0.1	0.5	2	1	2	0.48	22904	47716.66667	0.498066263	0.42555	17.04059757		
	0.1	0.1	1	0.25	1	0.25	0.115	6004.3	52211.30435	0.544981262	0.52384	4.035824391		
	0.1	0.1	1	0.5	1	0.5	0.14	7859.1	56136.42857	0.585951684	0.5674	3.269595374		
	0.1	0.1	1	1	1	1	0.19	8163	42963.15789	0.448449169	0.42555	5.381075948		
	0.1	0.1	1	1.5	1	1.5	0.24	6026.8	25111.66667	0.262115417	0.243173	7.789687525		
	0.1	0.1	1	2	1	2	0.29	4201	14486.2069	0.151206935	0.14185	6.596359105		
	0.1	0.2	2	0.25	1	0.25	0.205	33913	165429.2683	0.431687412	0.43548	-0.870898228		
	0.1	0.2	2	0.5	1	0.5	0.23	37178	161643.4783	0.421808399	0.42555	-0.87923879		
	0.1	0.2	2	1	1	1	0.28	31718	113278.5714	0.295600252	0.291615	1.366614168		
	0.1	0.2	2	1.5	1	1.5	0.33	16652	50460.60606	0.131676871	0.127953	2.910343038		
	0.1	0.2	2	2	1	2	0.38	10655	28039.47368	0.073168962	0.070736	3.439496106		
	T	0.2	0.1	0.5	0.25	1	0.25	0.18	20413	113405.5556	1.183726467	1.15264	2.696979728	
0.2		0.1	0.5	0.5	1	0.5	0.28	32944	117657.1429	1.228104508	1.20272	2.110591686		
0.2		0.1	0.5	1	1	1	0.48	56661	118043.75	1.232139911	1.21928	1.054713538		
0.2		0.1	0.5	1.5	1	1.5	0.68	51508	75747.05882	0.790647318	0.733707	7.760634411		
0.2		0.1	0.5	2	1	2	0.88	41670	47352.27273	0.494262721	0.42555	16.14680328		
0.1		0.1	1	0.25	1	0.25	0.14	8531.2	60937.14286	0.636061509	0.61904	2.74966227		
0.1		0.1	1	0.5	1	0.5	0.19	12666	66663.15789	0.695829618	0.68088	2.195631805		
0.1		0.1	1	1	1	1	0.29	12491	43072.41379	0.449589581	0.42555	5.64906146		
0.1		0.1	1	1.5	1	1.5	0.39	8959.4	22972.82051	0.239790154	0.21964	9.174173331		
0.1		0.1	1	2	1	2	0.49	6800.9	13879.38776	0.144872961	0.125163	15.74743419		
0.1		0.2	2	0.25	1	0.25	0.23	38889	169082.6087	0.441220798	0.4452	-0.893800907		
0.1		0.2	2	0.5	1	0.5	0.28	45169	161317.8571	0.420958692	0.42555	-1.078911634		
0.1		0.2	2	1	1	1	0.38	37142	97742.10526	0.255057868	0.265683	-3.999176399		
0.1		0.2	2	1.5	1	1.5	0.48	21295	44364.58333	0.11576931	0.115627	0.123076461		
0.1		0.2	2	2	1	2	0.58	13978	24100	0.062888912	0.062805	0.133606647		
Cruciform		0.2	0.1	0.5	0.25	1	0.25	0.26	27153	104434.6154	1.090087851	1.0368	5.139646096	
	0.2	0.1	0.5	0.5	1	0.5	0.36	41425	115069.4444	1.201094129	1.13184	6.118720735		
	0.2	0.1	0.5	1	1	1	0.56	64701	115537.5	1.20597969	1.16648	3.386229483		
	0.2	0.1	0.5	1.5	1	1.5	0.76	53220	70026.31579	0.730934239	0.713831	2.395978675		
	0.2	0.1	0.5	2	1	2	0.96	40329	42009.375	0.438493589	0.42555	3.04161412		
	0.1	0.1	1	0.25	1	0.25	0.23	12263	53317.3913	0.556526591	0.52384	6.239804349		
	0.1	0.1	1	0.5	1	0.5	0.28	15945	56946.42857	0.594406459	0.5674	4.759686112		
	0.1	0.1	1	1	1	1	0.38	16137	42465.78947	0.44325764	0.42555	4.161118613		
	0.1	0.1	1	1.5	1	1.5	0.48	11624	24216.66667	0.252773413	0.243173	3.947976355		
	0.1	0.1	1	2	1	2	0.58	8183.2	14108.96552	0.147269292	0.14185	3.820438684		
	0.1	0.2	2	0.25	1	0.25	0.41	70329	171534.1463	0.447618082	0.43548	2.787288039		
	0.1	0.2	2	0.5	1	0.5	0.46	76788	166930.4348	0.435604704	0.42555	2.362755014		
	0.1	0.2	2	1	1	1	0.56	64701	115537.5	0.301494922	0.291615	3.388002132		
	0.1	0.2	2	1.5	1	1.5	0.66	33918	51390.90909	0.134104496	0.127953	4.807621161		
	0.1	0.2	2	2	1	2	0.76	21667	28509.21053	0.07439474	0.070736	5.172386773		

References

[1] Lundquist, E. E., Stowell, Z. E., and Schuette, E. H., "Principles of Moment Distribution Applied to Stability of Structures Composed of Bars or Plates," NACA-WR-L-326, Jan. 1943.

[2] Kroll, W. D., Fisher, G. P., and Heimerl, G. J., "Charts for Calculation of the Critical Stress for Local Instability of Columns with I-, Z-, Channel, and Rectangular-Tube Section," NACA-WR-L-429, Nov. 1943.

[3] Van Der Maas, C. J., "Charts for Calculation of the Critical Stress for Local Instability of Columns with Hat Sections," *Journal of the Aeronautical Sciences*, Vol. 21, No. 6, June 1954, pp. 399-403
doi: 10.2514/8.3049

[4] Lundquist, E. E. and Stowell, Z. E., "Critical Compressive Stress for Outstanding Flanges," NACA-TR-734, Jan. 1942.

[5] Dassault Systèmes, *Abaqus/CAE*, 2024 Learning Edition, Dassault Systèmes, 2024.

[6] MathWorks, Inc., *MATLAB*, Version R2021b, Natick, MA, 2021.

[7] Bruhn, E. F., *Analysis and Design of Flight Vehicle Structures*, Jacobs Publishing, Carmel, IN, 1973.